

Article

# Energy Dissipation in Circular Drop Manholes under Different Outflow Conditions

Feidong Zheng<sup>1,2</sup>, Yun Li<sup>1,3,\*</sup>, Jianjun Zhao<sup>1</sup> and Jianfeng An<sup>1</sup>

<sup>1</sup> Nanjing Hydraulic Research Institute, Nanjing 210029, China; feidongzheng@126.com (F.Z.); jjzhao@nhri.cn (J.Z.); jfan@nhri.cn (J.A.)

<sup>2</sup> College of Water Conservancy and Hydropower Engineering, Hohai University, Nanjing 210098, China

<sup>3</sup> State Key Laboratory of Hydrology-Water Resources and Hydraulic Engineering, Nanjing 210029, China

\* Correspondence: yli\_nhri@126.com; Tel.: +86-025-8582-8022

Received: 3 September 2017; Accepted: 26 September 2017; Published: 30 September 2017

**Abstract:** Circular drop manholes have been an important device for energy dissipation and reduction of flow velocities in urban drainage networks. The energy dissipation in a drop manhole depends on the manhole flow patterns, the outflow regimes in the exit pipe and the downstream operation conditions, and is closely related to the hydraulic and geometric parameters of the manhole. In the present work, the energy dissipation of a drop manhole with three drop heights was experimentally investigated under free outflow conditions and constrained outflow conditions. The results demonstrate that the local head loss coefficient is solely related to the dimensionless drop parameter for free surface outflow without a downstream backwater effect, whereas it depends on the dimensionless submerge parameter for constrained outflow. Moreover, it is concluded that the energy dissipation is largely promoted when outlet choking occurs.

**Keywords:** drop manhole; energy dissipation; free outflow conditions; constrained outflow conditions; outlet choking

## 1. Introduction

Drop manholes are hydraulic features that are widely implemented in urban drainage networks for steep catchments. The energy dissipation of plunge flow in drop manholes is one of the major concerns for urban system drainage designers. As pointed out by Christodoulou [1] and Granata et al. [2], adequate energy dissipation in drop manholes should be achieved in order to avoid excessive flow velocities—and, thus, erosion—in the exit pipe. However, this cannot be always attained, because of the wide range of discharges experienced in sewer systems during a flood event [3].

The energy dissipation of a drop manhole is related to many factors, which can be grouped into four categories: (a) the approach flow conditions associated with the filling ratio of the upstream pipe and the approach flow Froude number; (b) the outlet flow conditions, such as free outflow conditions, including free surface flow and pressurized flow (in the condition of outlet choking), and constrained outflow conditions, in which backwater effects downstream of the exit pipe are imposed on the outlet flow; (c) manhole configurations and dimensions, such as inlet or outlet entrance configurations, baffles in the manhole, drop height, and manhole diameter, etc.; and (d) air supply conditions. In the hydraulic studies of circular drop manholes [1,2,4–7] and rectangular drop manholes [3,8–10], the energy dissipation was investigated under free surface outflow conditions for different approach flow conditions or manhole configurations. In some other studies, the interest has been focused on the effects of ventilation absence on the sub-atmospheric pressure and pool depth, which can strongly influence the interaction between water and airflow and the dissipation energy in drop manholes [11]. However, the energy dissipation of a circular drop manhole has not yet been investigated under

constrained outflow conditions or outlet choking, although the drop manhole has to operate under surcharged conditions in many instances, i.e., severe rain events.

This work aims to investigate the energy dissipation of the flow inside the circular drop manhole and its relation to the outflow conditions. Results of laboratory experiments are presented and analyzed for three manhole models of different drop heights.

## 2. Experimental Set-Up and Experiments

The experimental arrangement is schematically shown in Figure 1. The experimental facility consisted of a head tank, plexiglass circular manhole models and a downstream pool. The plunge flow was created by the flow from the upstream horizontal inlet pipe with an internal diameter  $D_{in} = 200$  mm. The inflow pipe was connected to the manhole with a straight inlet entrance, and the flow to this pipe was provided from a head tank. A manhole model with an internal diameter of  $D_M = 0.54$  m with drop heights of  $s = 0.93, 1.50$  and  $2.40$  m was used in the tests performed. The lower part of the vertical dropshaft was connected to a horizontal outlet pipe with an internal diameter  $D_{out} = 200$  mm. The shaft pool height  $P$  was 35 mm. The flow from the outlet pipe was drained into a downstream pool that was connected to the laboratory sump. The pool was considered to be a pressurized system downstream from the manhole, which allowed for analyzing a wide range of back pressures from the exit pipe, taking into account the various work conditions.

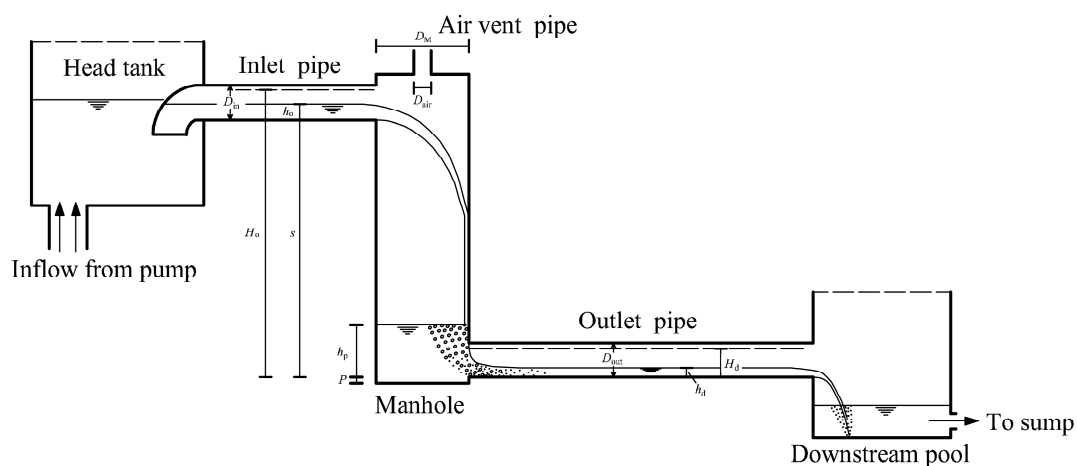


Figure 1. Sketch of experimental setup.

A pump was used to supply water from the main laboratory sump, and the discharges were measured with an ultrasonic flowmeter. Flow depths were recorded with piezometers in the upstream and downstream pipes, while the time-average pool depth  $h_p$  was measured by using a set of piezometers connected to the manhole bottom. The approach flow depth  $h_o$  was measured 1.2 m from the manhole inlet, where the flow has a horizontal surface and the pressure distribution is almost hydrostatic. The downstream flow depth  $h_d$  was recorded 2 m from the manhole outlet, where the flow is gradually varied and the air entrained by the manhole almost detrained. The air demand tests were performed by connecting the inlet pipe to the head tank with a same diameter elbow and sealing the manhole with a plexiglass cover on the manhole top, thus the air was supplied only through a 50 mm diameter pipe fitted to the cover. The airflow into the manhole was calculated by measuring the mean airflow velocity with a thermal anemometer.

Overall, seven series of experiments were run to investigate the energy dissipation in circular drop manholes under different outflow conditions (see Table 1). The first three series were run under free surface outflow conditions without backwater effects from the downstream pool. In series four, experiments were performed to investigate the outlet choking, i.e., the sudden transition from free

surface to pressurized flow in the exit pipe. Series 5–7 were run under constrained outflow conditions, in which back pressures from the downstream pool were imposed on the outlet flow.

**Table 1.** List of experiments.

Series	$s$ (m)	Inflow Condition	Outflow Condition
1	0.93	Free surface	Free surface
2	1.50	Free surface	Free surface
3	2.40	Free surface	Free surface
4	0.93	Pressurized (full pipe)	Free surface, Pressurized
5	0.93	Free surface	Constrained (backwater effect)
6	1.50	Free surface	Constrained (backwater effect)
7	2.40	Free surface	Constrained (backwater effect)

### 3. Results and Discussion

#### 3.1. Flow Patterns

For a manhole under free outflow conditions, the energy dissipation is strongly related to the flow patterns describing the drop manhole flow and the outflow regimes in the exit pipe. Chanson [8–10] defined three basic flow regimes of the drop manhole flow for rectangular drop manholes, namely, flow Regimes R1, R2, and R3, based on the free falling nappe impact location. Regime R1 usually occurs at low flow rates with the falling jet directly impacting into the manhole pool. For Regime R2, the falling nappe impacts the manhole outlet zone. With increasing discharges, this flow regime transforms into Regime R3, with the falling jet impacting on the manhole inner sidewall. For Regime R3, a water veil spreads down the manhole wall beyond impingement, forming a water curtain at the manhole outlet. For larger discharges, a roller tends to form at the top of the impact region, as observed by Rajaratnam et al. [4]. At high flow rates, outlet choking occurs when the free surface flow in the exit pipe transits to pressurized flow [12].

The classification of drop manhole flow regimes was extended by de Marinis et al. [13] and Granata et al. [2,6], taking into account additional effects present for circular drop manholes. According to their investigations, three subregimes for Regime R2 and two subregimes for Regime R3 were proposed, as indicated in Figures 2 and 3, respectively. Regime R2a occurs if the jet impacts the zone between the manhole bottom and the manhole outlet. This flow regime transforms to Regime R2b, with the entire falling jet impacting the outlet pipe invert. Regime R2c can be observed if the jet partially impacts on the outlet pipe obvert. Compared with Regime R3a, the flow jet for Regime R3b impacts the manhole sidewall at a higher Froude number, leading to the formation of a radially spreading water jet. Based on the experimental observations of this study, different shapes of the free falling nappe before impingement were observed (see Table 2). For a manhole with large drop height at low flow rates, the side edges of the nappe intersect and form a ‘central ridge’, while for smaller drop height or high flow rates, the nappe usually exhibits with a shape of horseshoe. These were consistent with the earlier observations of Chanson [9].

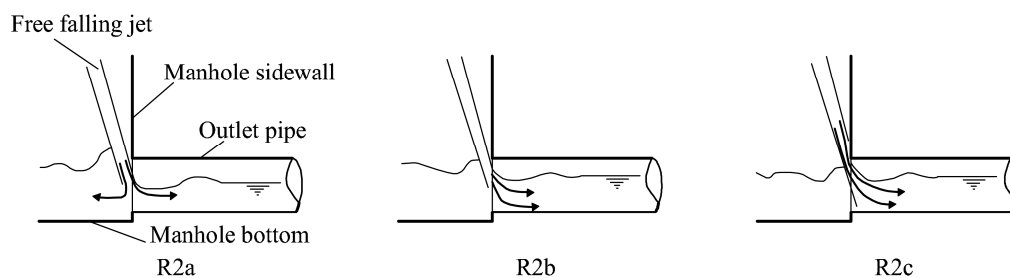


**Figure 2.** Regime R2 with subregimes.

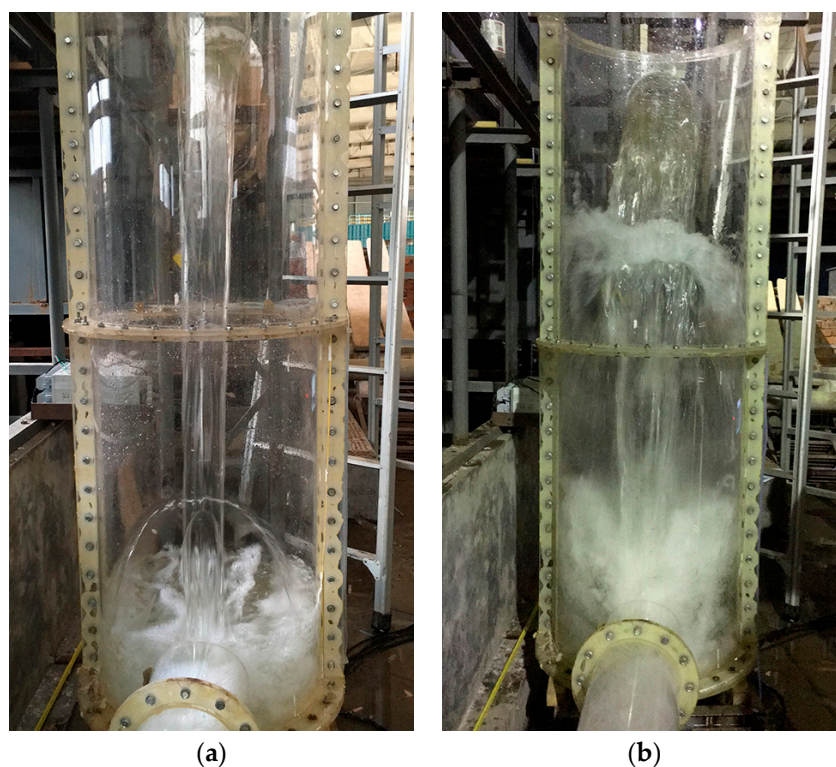


**Figure 3.** Regime R3 for  $s = 1.5$  m with Regimes (a) R3a; and (b) R3b.

**Table 2.** Shape of free flow jet before impingement.

$s$ (m)	Shape of Flow Jet for Different Regimes		
	R1	R2	R3
0.93	Central ridge, Horseshoe	Horseshoe	Horseshoe
1.50	Central ridge	Horseshoe	Horseshoe
2.40	Central ridge	Central ridge	Central ridge, Horseshoe

For a manhole under constrained outflow conditions, the energy dissipation also depends on the downstream operation conditions, i.e., water depths in the downstream pool. At low flow rates, no obvious hydraulic jump forms in the exit pipe in the variation range of water depths in the downstream pool. For large discharges, with the increase of water depth in the downstream pool a hydraulic jump starts in the exit pipe and then moves toward the outlet entrance until it becomes a critical hydraulic jump at the outlet entrance, and behaves as a submerged jump near the out entrance at last.

### 3.2. Energy Dissipation

#### 3.2.1. Definition

For a manhole under free outflow conditions, the energy dissipation in regime R1 was caused by the direct impact of the free falling nappe on the bottom of the shaft, inducing zones of large velocity gradients and increase of flow turbulence. A poor energy dissipation of the drop manhole may occur if the falling jet collided with the invert of downstream sewer (Regime R2). In this regime, most of the flowrate was conveyed to downstream pipe directly, causing undesirable downstream conditions. In regime R3, the energy dissipation occurred when the falling jet impinged on the inner side of the manhole, leading to the formation of a splash jet directed upwards, and a downward spreading jet. This energy dissipation was promoted by the frictional resistance of the spreading flow due to the roughness of the manhole wall, and by the mixing of the spreading jet with the water in the

manhole pool. The energy dissipation can vary within large limits when the free surface flow in the exit pipe transits to pressurized flow. For a manhole under constrained outflow conditions, the energy dissipation also depends on the water depth in the downstream pool. Figure 4 shows two definition sketches of drop manholes under free surface and pressurized outflow conditions. The relative energy loss is defined as

$$\eta = \frac{H_o - H_d}{H_o} \tag{1}$$

where the approach flow energy head is  $H_o = s + h_o + V_o^2/2g$ , and the outflow energy head is  $H_d = h_d + V_d^2/2g$  for free surface conditions, while  $H_d = p_d/\rho g + V_d^2/2g$  for pressurized conditions.

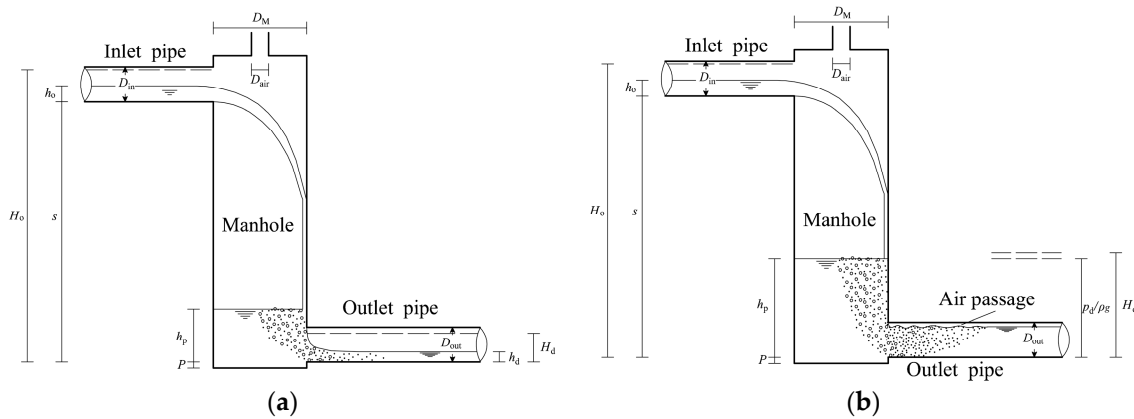


Figure 4. Definition sketch for (a) free surface outflow; and (b) pressurized outflow.

### 3.2.2. Free Outflow Conditions

#### (1) Free surface outflow

Plots of  $\eta$  versus the dimensionless flow rate  $Q^*$  for free surface outflow are presented in Figure 5 under different drop heights  $s$ , in which  $Q^*$  is defined by the equation

$$Q^* = \frac{Q_w}{\sqrt{gD_{in}^5}} \tag{2}$$

where  $Q_w$  = the volumetric flow rate and  $g$  = acceleration due to gravity.

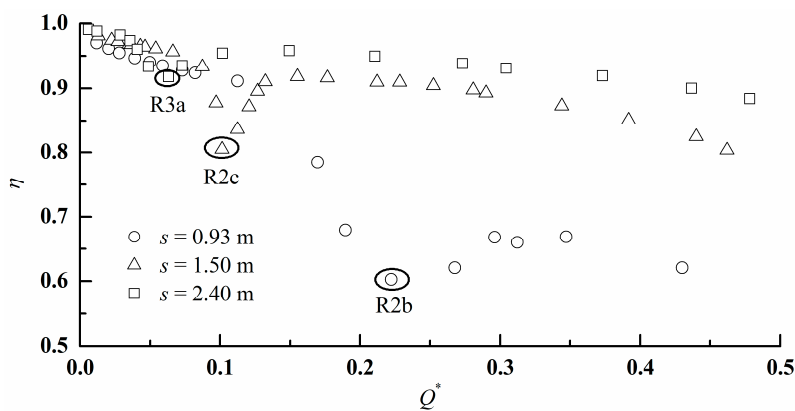


Figure 5. Variation of  $\eta$  with  $Q^*$  for free surface outflow.

It can be seen from this figure that the largest energy losses are observed in Regime R1 for each of the drop heights  $s$ . Values of  $\eta$  drop rapidly with an increase in  $Q^*$ , and pass through their

minimum values at different Regimes, i.e., at Regime R2 for  $s = 0.93$  m and  $s = 1.50$  m, and at Regime R3 for  $s = 2.40$  m. This may be attributed to the effect of the shape of the free-falling nappe before impingement; the nappe has a horseshoe shape for  $s = 0.93$  m and  $s = 1.50$  m, while the side edges of the nappe intersect for  $s = 2.40$  m. Subsequently, values of  $\eta$  increase first, and then decrease for different  $s$  at high flow rates.

The local head loss in a drop manhole is generally estimated regardless of flow regimes by

$$\Delta H = K \frac{V_o^2}{2g} \quad (3)$$

where  $K$  is the local head loss coefficient. Dissipative studies of circular drop manholes have convinced us that the local head loss coefficient was based solely on the drop parameter  $D = (gs)^{0.5}/V_o$  [1,6].

Granata et al. [6] found that the local head loss coefficient of a drop manhole under free surface outflow conditions,  $K_f$ , depends on the drop parameter  $D$  in the range  $0 < D < 8$  as

$$K_f = 0.25 + 2D^2 \quad (4)$$

It is shown in Figure 6 that the present test data agrees well with Equation (4), extending the range of agreement up to  $D = 21.6$ .

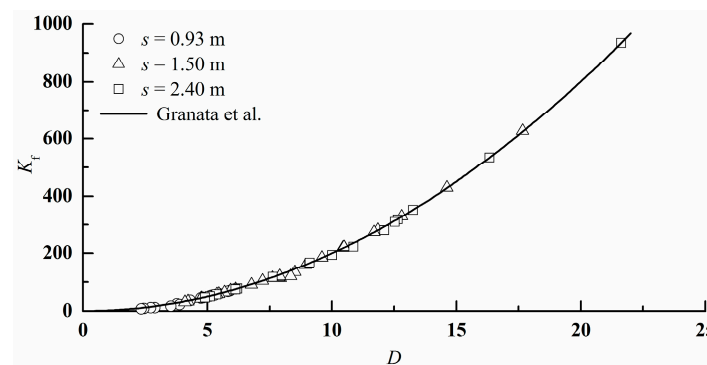


Figure 6.  $K_f$  versus  $D$  for entire present test range.

## (2) Pressurized outflow

Figure 7 shows that the energy dissipation for drop manhole increases notably when the free surface flow in the exit pipe shifts to pressurized flow, indicating a large dissipation effect in choking flow. This may be explained by the strong mixing mechanism between the entrained air and the water flow in the outlet pipe, which can be illustrated by the remarkable increase in dimensionless air demand  $Q_a/Q_w$  in Figure 8. The dimensionless pool height  $h_p/D_{out}$  is plotted as a function of  $Q^*$  in Figure 9. Once the flow in the exit pipe chokes, an abrupt drop in manhole pool height and large unsteady fluctuations in pool water surface illustrated by large standard deviations occur. These results indicate that the outlet choking is advantageous in promoting energy dissipation and reducing manhole pool height, which has to be smaller than the drop height to avoid undesired backwater effects to the approaching flow.

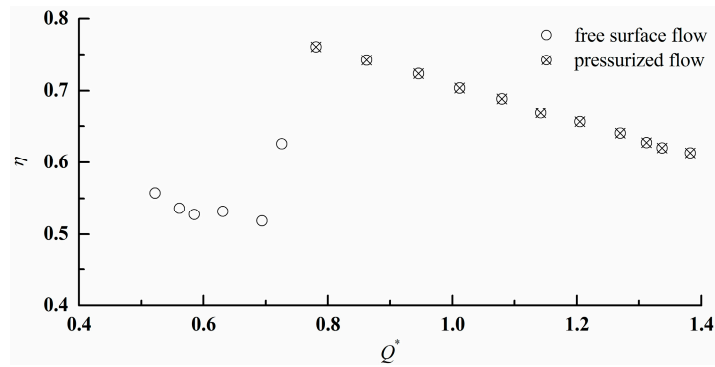


Figure 7. Variation of  $\eta$  with  $Q^*$  for  $s = 0.93$  m.

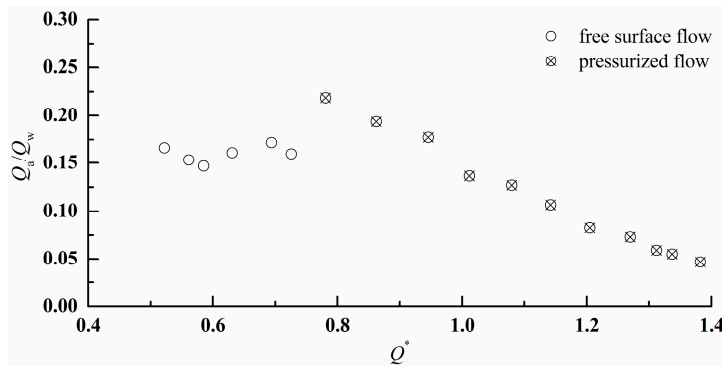


Figure 8. Variation of  $Q_a/Q_w$  with  $Q^*$  for  $s = 0.93$  m.

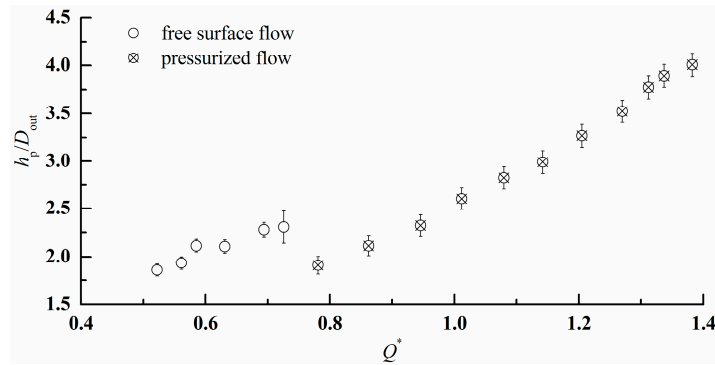


Figure 9. Variation of  $h_p/D_{out}$  with  $Q^*$  for  $s = 0.93$  m.

### 3.2.3. Constrained Outflow Conditions

For a drop manhole under constrained outflow conditions, the energy dissipation is difficult to estimate when the hydraulic jump passes the measuring location because of the uncertainty in the calculation of the residual energy in the exit pipe, given the unstable water depth and pressure. Hence, for a given large flow rate, the minimum water depth in the downstream pool is set to the value at which a critical hydraulic jump or submerged hydraulic jump occurs. The head loss coefficient of a drop manhole under constrained outflow conditions due to backwater effects from the downstream pool,  $K_c$ , can be calculated using Equation (3).

For a given drop height  $s$  and specified approach flow condition, if  $H_d$  is proportional to the manhole pool height  $h_p$ , that is

$$H_d = \alpha h_p \tag{5}$$

where  $\alpha$  is a dimensionless parameter, then  $K_c$  can be described by

$$K_c = \frac{2gH_o}{V_o^2} - \alpha \frac{2gD_{out}}{V_o^2} \frac{h_p}{D_{out}} \tag{6}$$

Equation (6) is evaluated with experimental results for different manhole drop heights  $s$  in Figure 10. It is apparent that a definite linear relationship exists between  $K_c$  and the dimensionless pool height  $h_p/D_{out}$  for each drop height  $s$  and drop parameter  $D$ , indicating that  $\alpha$  is approximately constant if the manhole configuration and approach flow condition remain unchanged.

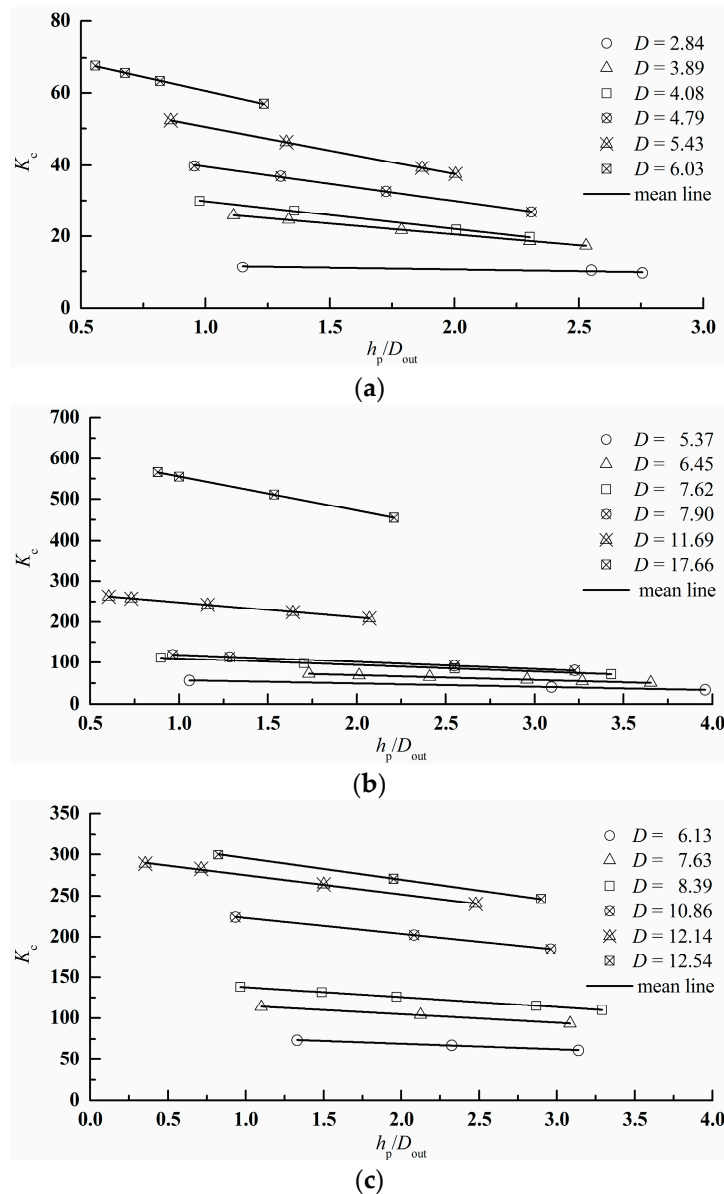


Figure 10. Variation of  $K_c$  with  $h_p/D_{out}$  for (a)  $s = 0.93$  m, (b)  $s = 1.50$  m and (c)  $s = 2.40$  m.

Equation (6) could be written in a different form:

$$C = \frac{2gH_o}{V_o^2} - K_c = \alpha \frac{2gh_p}{V_o^2} \tag{7}$$

where  $C$  is a dimensionless parameter. If  $\alpha$  is a constant for different  $s$  and  $D$ , then  $C$  will be a linear function of  $2gh_p/V_o^2$ . In Figure 11, experimental results for constrained outflow conditions are shown plotted with  $C$  against  $2gh_p/V_o^2$  for a number of discharges and three manhole drop heights. It is interesting that a definite linear relation appears to exist between these two parameters, indicating that  $\alpha$  is approximately constant. This can be seen in Figure 12, where  $\alpha$  is plotted against  $2gh_p/V_o^2$ , especially for  $2gh_p/V_o^2$  greater than 25. Using the data of Figure 11, the best fitting is

$$C = \frac{2gh_p}{V_o^2} - 0.36 \tag{8}$$

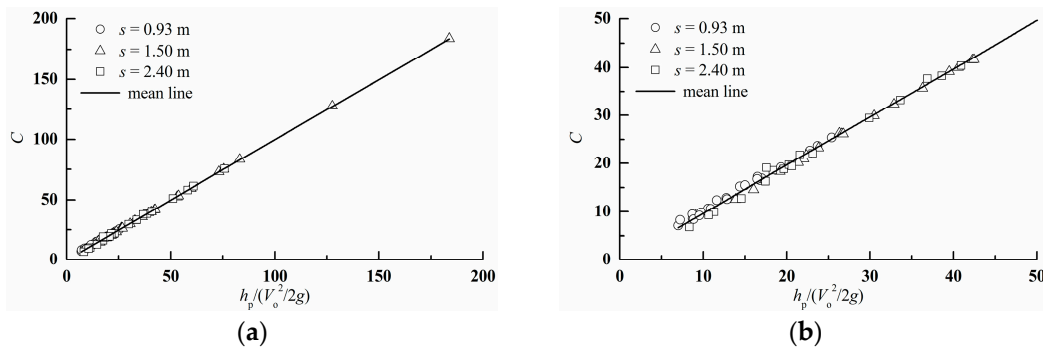


**Figure 11.** Rating curve between  $C$  and  $h_p/(V_o^2/2g)$  for (a) entire present test range; (b) test data for  $0 < h_p/(V_o^2/2g) < 50$ .

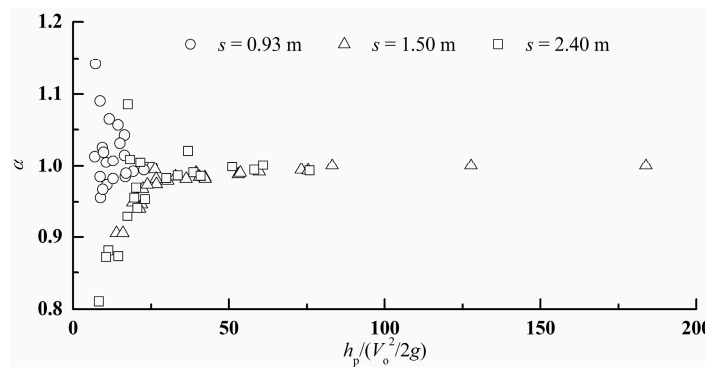


**Figure 12.** Variation of  $\alpha$  with  $h_p/(V_o^2/2g)$ .

Hence, Equation (7) reduces to

$$K_c = \frac{2g(s + h_o - h_p)}{V_o^2} + 1.36 \tag{9}$$

Combination of Equations (4) and (9) generates

$$K_c = K_f + \left[ 1.11 - \frac{2g(h_p - h_o)}{V_o^2} \right] \tag{10}$$

The head loss coefficient  $K_c$  can be considered as the sum of that for free surface outflow conditions ( $K_f$ ) and that due to the back pressure from the exit pipe (terms in brackets), which is related to the approach flow conditions and pool height. Similar to  $D$ , a dimensionless submerge parameter,  $D' = [g(s + h_o - h_p)]^{0.5}/V_o$ , can be defined for constrained outflow conditions, in which the term in parentheses is the difference in elevation between the water surfaces of the approach flow and

the manhole pool. Thus, the head loss coefficient for constrained outflow conditions can be solely characterized by the submerge parameter  $D'$ , for  $2.0 < D' < 16.8$  resulting in

$$K_c = 2D'^2 + 1.36 \quad (11)$$

#### 4. Conclusions

Drop manholes are effective energy dissipaters widely employed in urban drainage networks. In the present study, the hydraulic performance of circular drop manholes was investigated experimentally with respect to their energy dissipation in three models of different drop heights. It is concluded that the local head loss coefficient is solely dependent on the dimensionless drop parameter  $(gs)^{0.5}/V_o$  for free surface outflow without a downstream backwater effect, while it can be solely characterized by the dimensionless submerge parameter, defined as  $[g(s + h_o - h_p)]^{0.5}/V_o$ , for constrained outflow due to the downstream backwater effect. Based on experimental results, empirical equations for different outflow conditions are proposed for practical applications. Furthermore, the mixing between airflow and water flow is largely intensified when outlet choking occurs, resulting in abrupt increases in air demand and energy dissipation.

**Acknowledgments:** This research was supported by the National Natural Science Foundation of China (Grant No. 51509162).

**Author Contributions:** Feidong Zheng performed the research and wrote the article; Yun Li led the work performance; Jianjun Zhao and Jianfeng An collected data through review of papers.

**Conflicts of Interest:** The authors declare no conflict of interest.

#### References

1. Christodoulou, G.C. Drop manholes in supercritical pipelines. *J. Irrig. Drain. Eng. ASCE* **1991**, *117*, 37–47. [[CrossRef](#)]
2. Granata, F.; de Marinis, G.; Gargano, R.; Hager, W.H. Energy loss in circular drop manholes. In Proceedings of the 33rd IAHR Congress (CD-Rom), Vancouver, BC, Canada, 9–14 August 2009.
3. Carvalho, R.F.; Leandro, J. Hydraulic characteristics of a drop square manhole with a downstream control gate. *J. Irrig. Drain. Eng. ASCE* **2011**, *138*, 569–576. [[CrossRef](#)]
4. Rajaratnam, N.; Mainali, A.; Hsung, C.Y. Observations on flow in vertical dropshafts in urban drainage systems. *J. Environ. Eng. ASCE* **1997**, *123*, 486–491. [[CrossRef](#)]
5. Jalil, A. Experimental and Numerical Study of Plunging Flow in Vertical Dropshafts. Ph.D. Thesis, University of Alberta, Edmonton, AB, Canada, 2009.
6. Granata, F.; de Marinis, G.; Gargano, R.; Hager, W.H. Hydraulics of circular drop manholes. *J. Irrig. Drain. Eng. ASCE* **2011**, *137*, 102–111. [[CrossRef](#)]
7. Granata, F.; de Marinis, G.; Gargano, R. Flow-improving elements in circular drop manholes. *J. Hydraul. Res.* **2014**, *52*, 347–355. [[CrossRef](#)]
8. Chanson, H. Hydraulics of Roman aqueducts: Steep chutes, cascades, and dropshafts. *Am. J. Archaeol.* **2000**, *104*, 47–72. [[CrossRef](#)]
9. Chanson, H. An experimental study of Roman dropshaft hydraulics. *J. Hydraul. Res.* **2002**, *40*, 3–12. [[CrossRef](#)]
10. Chanson, H. Hydraulics of rectangular dropshafts. *J. Irrig. Drain. Eng. ASCE* **2004**, *130*, 523–529. [[CrossRef](#)]
11. Granata, F.; de Marinis, G.; Gargano, R. Air-water flows in circular drop manholes. *Urban Water J.* **2015**, *12*, 477–487. [[CrossRef](#)]
12. Camino, G.A.; Rajaratnam, N.; Zhu, D.Z. Choking conditions inside plunging flow dropshafts. *Can. J. Civ. Eng.* **2014**, *41*, 624–632. [[CrossRef](#)]
13. De Marinis, G.; Gargano, R.; Granata, F.; Hager, W.H. Circular drop manholes: Preliminary experimental results. In Proceedings of the 32nd IAHR Congress (CD-Rom), Venice, Italy, 1–6 July 2007.

